

# Fractographic Investigation on Some Sinter-hardened Steels

B. Rivolta, M.R. Pinasco, G.F. Bocchini

**A** short description of the basic concepts of sinter-hardening explains the big application potential of this new technique of powder metallurgy. Sinter-hardened steels can compete advantageously with conventional high hardness steels, usually obtained by adding a heat-treating step to a controlled sintering process. The reliability of possible new materials calls for suitable investigation methods. In addition to microstructure investigations and mechanical testings, the observation of rupture surfaces may significantly contribute to differentiate grades of ferrous powders formulated for sinter-hardening applications, which have been investigated. Whereas two powders are hybrid grades, with a Mo-alloyed basis and nickel and copper additions by diffusion bonding, the other two are completely alloyed, containing nickel and copper. The partial and uneven diffusion of nickel brings about the presence of various microstructures: some of these are characterized by different yielding responses, when stressed by external actions. The fractographic investigations, carried out at SEM, are apt to distinguish and assess the shares of plastically deformed areas. The influence of different alloying methods is clearly detected. The results of the investigation represent a sound basis to suggest possible application condition and selection criteria among different alloying techniques.

**Parole chiave:** acciaio, sinterizzazione, frattura, metallurgia delle polveri, metallografia

## INTRODUCTION

Sinter-hardening is a process of powder metallurgy in which the cooling rate in the sintering furnace is fast enough that a significant portion of the material matrix transforms to martensite [1,2]. It is a relatively new technique which is becoming more and more important in industrial equipment because it offers good manufacturing economy by providing a one-step process together with good combination of strength, toughness and hardness [3, 4, 5]. That's why sinter-hardened steels can compete advantageously with conventional high hardness steels, usually obtained by adding a heat-treating step to a controlled sintering process.

By sinter-hardening, a great variety of microstructures and properties can be obtained by varying the alloying elements, their contents, the different alloying methods, as well as the post sintering cooling rate. By controlling these variables, the microstructure can be varied, to produce the required portion of martensite which will lead to the desired mechanical properties.

In this study the effect of different elements contents and alloying methods have been investigated through microstructure and fractographic analysis. The powders analyzed differ both for alloying method and for alloying elements contents. While two powders are hybrid grade with a Mo-alloyed basis and different nickel and copper additions by diffusion-bonding, the other two are completely alloyed grades with different nickel and copper contents.

In order to characterize these sinter-hardened steels, an extended experimental program has been set up, in which physical, microstructural and mechanical properties have been studied [6]. In this work the fractographic investigation is described: through the use of an image-analysis software, a calculation of the areas characterized by presence of dim-

ples has been carried out.

Moreover, a shape factor of the areas has been calculated, in order to have a measure of the homogenization degree of the sinter-hardened steels [7]. The obtained results have been related to the microstructures.

## MATERIALS AND METHODS

With four different grades of ferrous powders, formulated for sinter-hardening applications, gears have been pressed in industrial equipment, at density of 7.0 g/cm<sup>3</sup>.

The powders differ for both alloying grade and alloying contents and are described in Table 1.

The utilized forces to press the samples vary from a minimum value of 920 KN for Distaloy to a maximum value of 1415 KN for Atomet 4701.

The samples were sinter-hardened at 1120°C under endogas atmosphere, after 20-25 minutes soaking time they were fast cooled (about 8°C/s in the temperature range 850°C - 400°C). Afterwards, a treatment of stress relieving in air for an hour at 180°C was carried out.

The gears so obtained have been subjected to a mechanical test as reported in Figure 1, whose results are summarized in Table 2 and widely reported in [6], where R is the rupture strength and Δl<sub>max</sub> is the maximum displacement of the load application point.

On these samples a fractographic analysis has been carried out at SEM, on different positions of the sample surface, in order to obtain information about distribution and morphology of the areas characterized by presence of dimples. Through an image analysis software (ImageProPlus, ver.4.1), the areas of surface characterized by presence of dimples have been measured and for each material the hydraulic diameter of the area has been evaluated. The hydraulic diameter is defined as follows:

$$D_H = 4A / p \quad (1)$$

where A is area and p is perimeter of each zone interested by the dimples. This parameter can be considered as a shape factor pointing out the homogenization degree of the sinter-

B. Rivolta, Dipartimento di Meccanica, Politecnico di Milano, Italy

M. R. Pinasco, Dip. di Chimica e Chimica Industriale, University of Genova, Genova, Italy

G. F. Bocchini, Powder Metallurgy Consultant, Rapallo (GE), Italy

Paper presented at the 7<sup>th</sup> European Conference EUROMAT 2001, Rimini, 10-14 June 2001, organised by AIM

Commercial designation	Fe (a)	Ni(b)	Ni(c)	Mo	Cr	Mn	Cu(b)	Cu (d)
Distaloy DH-I	96.50			1.50			2.0	
Distaloy HP-I	92.50	4.0		1.50			2.0	
Mannesmann MSP 4	95.25		4.0	0.55		0.20		1.0
Atomet 4701	97.20		0.90	1.00	0.45	0.45		1.0

(a) before copper, graphite and lubricant addition; (b) added by diffusion-bonding;  
 (c) added before atomization; (d) added by mixing

Table 1: List of sinter-hardened steels to be investigated.

Tabella 1: Acciai da sinterotempra considerati.

Commercial designation	Carbon content, %	R [N/mm <sup>2</sup> ]	Δl <sub>max</sub> [mm]
Distaloy DH-I	0.71	990	0.82
Distaloy HP-I	0.58	920	1.00
MSP 4	0.55	699	0.67
Atomet 4701	0.82	675	0.68

Table 2: Results of the mechanical test.

Tabella 2: Risultati delle prove meccaniche.

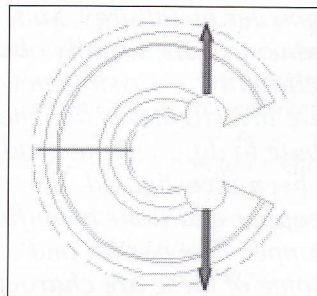


Figure 1: Schematic representation of the mechanical tests.

Figura 1: Rappresentazione schematica delle prove meccaniche effettuate.

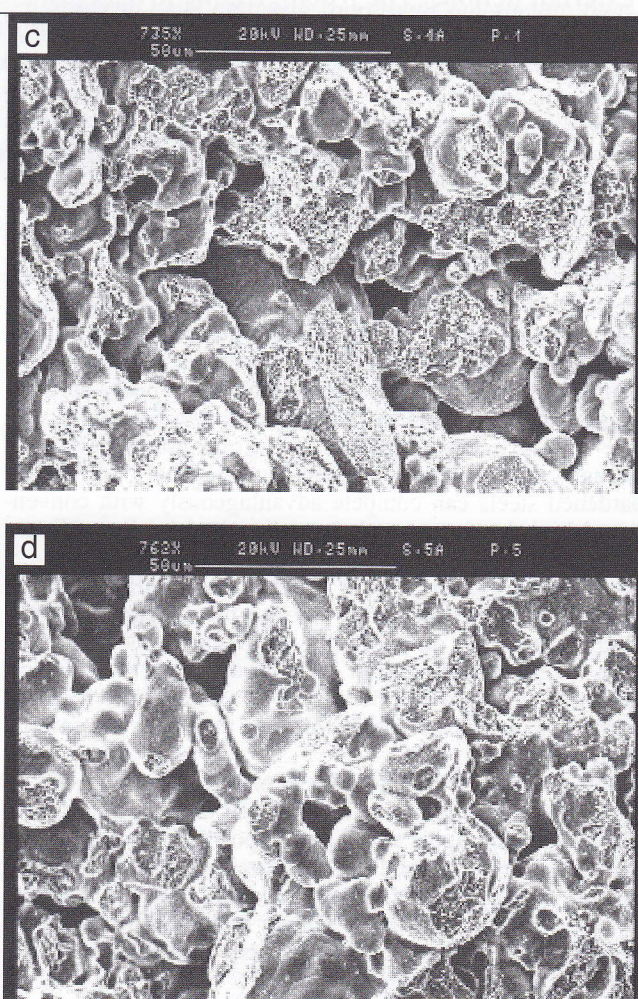
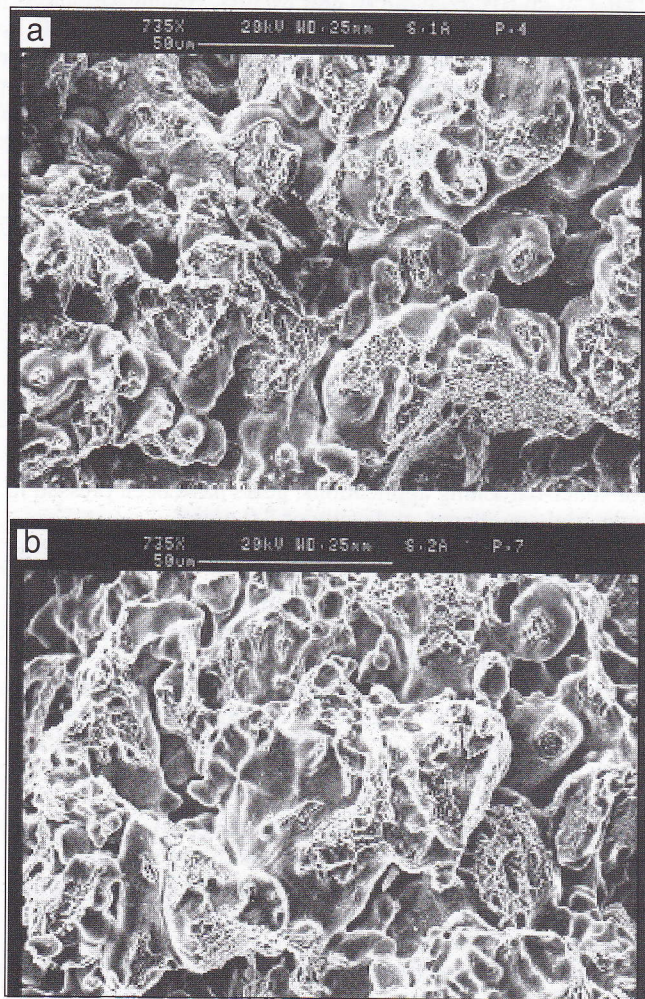


Figure 2: SEM images for Distaloy DH-1 a), Distaloy HP-1 b), MSP 4 c) and Atomet 4701 d).

Figura 2: Frattografie di materiali da polvere Distaloy DH-1 a), Distaloy HP-1 b), MSP 4 c) e Atomet 4701 d).

red materials [7]. In fact it represents a useful index of the sintering degree of the material because during the sintering process the diffusive phenomena tend to increase the necks corresponding to contacts formed during pressing, between powder grains [7].

Moreover on each material a complete microstructure analysis has been carried out.

## RESULTS

In Figure 2 examples of the SEM images are shown for the four sinter-hardened materials.

The values of ductile areas are shown in Figure 3. They are calculated as ratios between the sum of the areas interested by dimples and the total area of the surface.

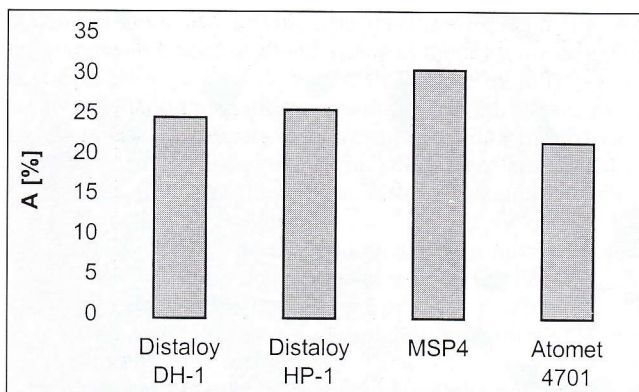


Figure 3: Fraction of the area interested by the presence of dimples for each powder.

Figura 3: Frazione di area di frattura interessata dalla presenza di microcavità per ciascun tipo di materiale.

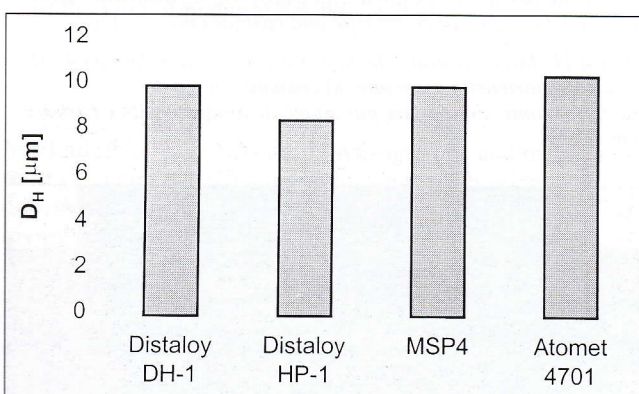


Figure 4: Mean hydraulic diameter of the ductile areas calculated for each material.

Figura 4: Diametro idraulico medio delle aree duttili calcolato per ciascun materiale.

It can be noted that while the material showing the maximum percentage of ductile area is the pre-alloyed material with 4% of nickel content, the minimum of dimples area is verified for the pre-alloyed material with 0.9% of nickel content. On the other side, the ductile areas of the diffusion-bonded powders show similar value and intermediate in comparison to the pre-alloyed ones.

Moreover, the diffusion-bonded material with 4% nickel shows a value of ductile area smaller than pre-alloyed material with the same nickel content even if it could be expected that both materials should show similar values because of the same nickel content. With regard to this matter, more information can be deduced from the analysis of the shape of the areas through the calculation of the hydraulic diameter, whose results are reported in Figure 4.

While Distaloy DH-1, MSP 4 and Atomet 4701 materials present a similar value of hydraulic diameter, the diffusion bonded powder with 4% of nickel content is the only one that shows a lower one (equal to 8.6 mm).

This value for this material could be related to an inadequate nickel diffusion. In fact the analysis of the sintering cycle shows that the material is kept at sintering temperature of 1120°C for a time interval of about 20 minutes which probably is not sufficient to enhance enough the diffusion of the elements. On the other side this material exhibits the highest rupture elongation. As the elongation is localized in a few areas, it could be thought that hydraulic diameter is lower because a concentrated necking could have been.

These results are confirmed by the microstructure analysis. The Distaloy DH-1 microstructure is mainly formed by mar-



Figure 5: Distaloy DH-1 LOM-micrograph. Martensite, transforming austenite, very fine pearlite (dark, not resolved), upper bainite.

Figura 5: Microstruttura del materiale da polvere Distaloy DH-1. Sono visibili martensite, austenite in via di trasformazione, perlite finissima (scura, non risolta), bainite superiore.



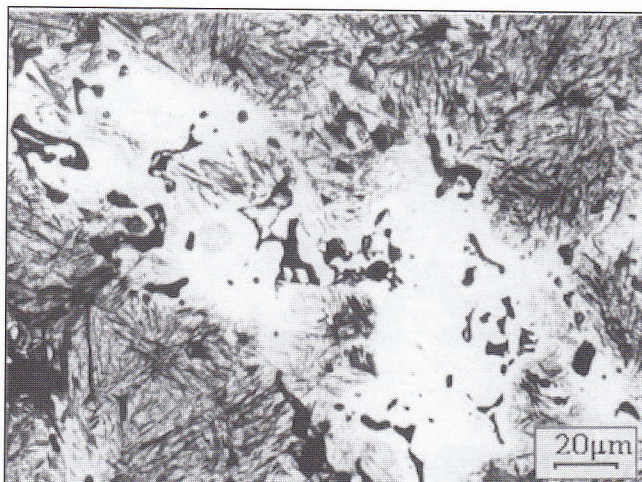
Figure 6: Distaloy DH 1 SEM micrograph: martensite with upper bainite.

Figura 6: Micrografia SEM del materiale da polvere Distaloy DH-1: è visibile martensite con bainite superiore.



Figure 7: Distaloy DH-1 SEM micrograph: very fine pearlite on a background of martensite.

Figura 7: Micrografia SEM del materiale da polvere Distaloy DH-1: perlite finissima su un fondo di martensite.



**Figure 8:** Distaloy HP-1 LOM micrograph. Wide areas of residual and transforming austenite and martensite needles. Little dark island of very fine perlite, not resolved.

**Figura 8:** Microstruttura del materiale da polvere Distaloy HP-1. Ampie isole di austenite residua ed in via di trasformazione con aghi di martensite. Piccole isole scure di perlite finissima, non risolta.



**Figure 9:** MSP 4 LOM-micrograph - Thin martensite associated with transforming austenite.

**Figura 9:** Microstruttura del materiale da polvere MSP 4. Martensite fine associata ad austenite in via di trasformazione.



**Figure 10:** MSP 4 SEM micrograph: martensite with some islands of transforming austenite.

**Figura 10:** Micrografia SEM del materiale da polvere MSP 4: martensite con alcune isole di austenite in via di trasformazione.

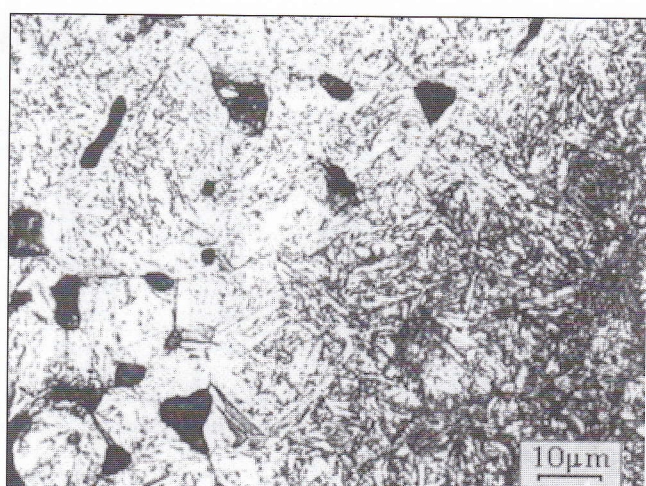


**Figure 11:** Atomet 4701 LOM micrograph. Background of martensite needles associated with transforming austenite. More attached dark zone of martensite and carbides not resolved.

**Figura 11:** Microstruttura del materiale da polvere Atomet 4701. Fondo di martensite associato ad austenite in via di trasformazione. Zone scure più attaccate di martensite e carburi non risolte.

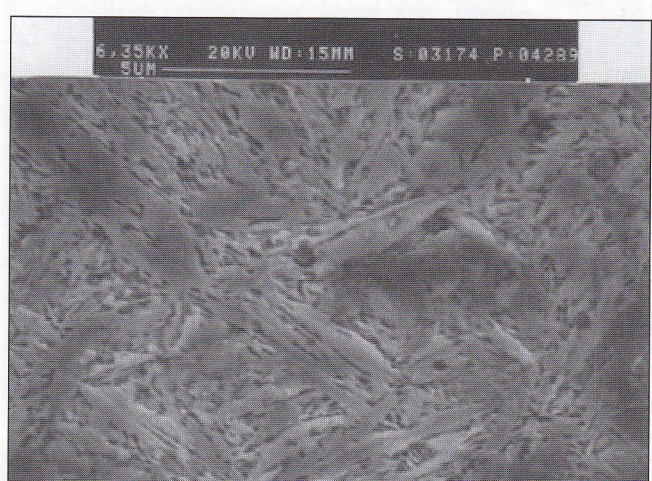


**Figure 12:** Atomet 4701 SEM micrograph: detail of Figure 11. More attacked zones: martensite with carbides.

**Figura 12:** Micrografia SEM del materiale da polvere Atomet 4701: dettaglio di Figura 11. Zone più attaccate: martensite e carburi.

tensite with different morphologies: big needles are visible on a background of small and sharp needles (Figure 5). A few transforming austenite is also present together, with upper bainite and very fine pearlite (dark in LOM micrograph) which only SEM observation has been able to identify (Figures 6 and 7).

Distaloy HP-1 has high nickel content so that the greater quantity of austenite areas (residual or transforming) and their localization around pores appear justified. Martensite is still the main phase present, while some fine pearlite is visible in very small quantity (Figure 8). The EDS microanalysis pointed out the noticeable chemical heterogeneity of the matrix especially for nickel. The highest nickel and copper content are present around pores, in the residual austenitic zones followed by transforming austenite and martensite areas. Nickel and copper elements are practically absent in the fine pearlite.

MSP 4 microstructure appears uniform and mainly constituted by thin martensite; small quantities of transforming austenite, homogeneously distributed, are visible often asso-

ciated to islands of very fine pearlite (Figures 9 and 10). The regular arrangement of the phases and the alloying amounts in the structure are consistent with the use of fully pre-alloyed powders and with the results achieved by means of fractographic investigation. Nevertheless, EDS microanalysis showed some difference of nickel content among different phases, a little higher in transformed austenite and martensite than in very fine pearlite.

Atomet 4701, fully pre-alloyed too, shows a microstructure constituted by zones of martensite, where (Cr, Fe)-carbides were evidenced, on a background of light martensite associated with austenite almost completely transformed (Figures 11 and 12). No residual austenite was found.

As regard to other interesting parameters, the porosity of all the examined materials is comparable and ranges from 9 to about 10%. As far as pore roundness, all alloys show a similar good behavior; the roundness index (defined as  $R = p^2/4pS$  with  $p$  = pore perimeter and  $S$  = pore area) has the value highest frequency in the range 1.25÷1.6. No marked influence of the kind of material has been noted.

## CONCLUSIONS

In addition to microstructural investigations and mechanical testings, a complete fractographic analysis has been carried out on some sinter-hardened steels, different both for alloying elements and for alloying technique.

From the fractographic analysis, carried out on SEM images, the maximum quantity of dimples area appears to be in the completely pre-alloyed material with high nickel content. On the contrary the nickel free pre-alloyed material shows the minimum value of dimples area, while the diffusion-bonded material shows an intermediate behavior. With regard to this matter, it seems not to be justified that the high nickel content material shows values of the ductile area lower than the pre-alloyed one with the same nickel content. Further information have been obtained from the calculation of the hydraulic diameter of each area. The low value of the hydraulic diameter in the 4% of nickel diffusion-bonded material can be justified by the analysis of the sintering cycle and by the higher elongation which could have increased the necking so influencing the hydraulic diameter. The sintering time of about 20 minutes at 1120°C is probably not enough to assure an adequate diffusion of the diffusion-bonded elements. These results seem to be confirmed by the microstructural analysis which shows a martensitic structure together with a great quantity of austenite areas (residual or transforming) in the Distaloy HP-1 material. Moreover, a noticeable chemical heterogeneity of the matrix especially

for nickel has been pointed out by EDS microanalysis on this material. Anyhow in-homogeneity is a peculiar feature of P/M steels from diffusion-bonded powders.

In the pre-alloyed materials microstructure appears more uniform and mainly constituted by martensite, with small quantity of transforming austenite homogeneously distributed and no residual austenite.

## AKNOWLEDGEMENTS

The authors warmly thank the company mG Minigears (Padova) for the helpfulness and the care shown when preparing the sample gears for the present investigation.

## BIBLIOGRAPHY

1. Rutz H.G., Graham A.H., Davala A.B., Sinter-hardening P/M steels, PM2TEC '97, International Conference on Powder Metallurgy & Particulate Materials, June 29-July 2, 1997, Chicago, IL, USA;
2. Julien B., L'Esperance G., Evaluating hardenability and compressibility for the development of an optimum sinter hardening powder, 1996 World Conference on Powder Metallurgy and Particulate Materials, Metal Powder Industries Federation, Washington D.C., June 1996;
3. Duchesne E., L'Esperance G., de Rege A., Sinter-hardening: predictability, powder design and process optimization, Domfer report, 1998;
4. V.C.Potter, W.B.James, T.F.Murphy, Improved dimensional control and elimination of heat treatment for automotive parts, Advances in Powder Metallurgy, Vol.3, L.F. Pease III and R.J.Sansoucy Editors, Metal Powder Industries Federation, 1990, 33-48;
5. W.B.James, What is sinter-hardening?, Hoeganaes Technical Data, Cinnaminson, N.J., USA, 1998;
6. G.F. Bocchini, M.G.Ienco, P.Piccardo, M.R.Pinasco, B.Rivolta, G.Silva, E.Stagno, Influenza della velocità di raffreddamento sulla struttura e le proprietà meccaniche di acciai da sinterotempra, Giornata di studio AIM "Innovazione nella Metallurgia delle Polveri: acciai per stampi e polveri da sinterotempra", Lecco, 12 Dicembre 2000;
7. B. Rivolta, M.R.Pinasco, Correlazione tra analisi frattografica e tenacità di acciai sinterizzati da polvere diffusion-bonded, La Metallurgia Italiana, Giugno 2001, pagg. 21-27.

## A B S T R A C T

### ABSTRACT

*Nell'ambito della Metallurgia delle Polveri la sinterotempra rappresenta un processo che ha avuto negli ultimi anni un interessante sviluppo dal punto di vista industriale, in quanto ha reso possibile l'ottenimento di pezzi meccanici, a partire da polveri, caratterizzati da un buon compromesso tra resistenza meccanica e tenacità con indubbi e considerevoli vantaggi dal punto di vista economico.*

*Nel processo di sinterotempra, successivamente alla fase di sinterizzazione, la velocità di raffreddamento che si raggiunge nel forno risulta tale da assicurare al pezzo elevate*

*caratteristiche meccaniche e di tenacità già a fine ciclo di sinterizzazione, senza quindi la necessità di ricorrere a trattamenti termici supplementari.*

*In questo lavoro sono stati presi in considerazione alcuni acciai commerciali da sinterotempra sui quali sono stati effettuati controlli microstrutturali, prove di resistenza meccanica ed una completa analisi frattografica.*

*Le polveri analizzate differiscono sia per metodo di alligazione sia per composizione chimica: mentre due polveri sono di tipo ibrido con base legata al Molibdeno e diversi quantitativi di nichel e rame aggiunti come elementi diffusion-bonded (Distaloy DH-1 e Distaloy HP-1), le altre due*

sono polveri completamente pre-legate con differente contenuto di nichel e rame (Mannesmann MSP 4 e Atomet 4701). Con le polveri sopra elencate, specifiche per il trattamento di sinterotempra, sono stati pressati ingranaggi in un impianto industriale. Le forze utilizzate per pressare i campioni variano da un valore minimo di 920 KN ad un valore massimo di 1415 KN per la polvere Atomet 4701. Gli ingranaggi sono stati poi sinterizzati in un impianto industriale in endogas ad una temperatura di 1120°C per venti-venticinque minuti, successivamente raffreddati ad una velocità di 8°C/s nell'intervallo di temperatura 850°C-400°C e sottoposti a distensione a 180°C per un'ora.

Gli ingranaggi così ottenuti sono stati sottoposti a prove meccaniche di tensio-flessione, analisi microstrutturale ed analisi frattografica effettuata, su immagini acquisite dal microscopio elettronico a scansione, in differenti posizioni della superficie di frattura al fine di ottenere informazioni riguardo la distribuzione e la morfologia delle aree caratterizzate dalla presenza di microcavità caratteristiche del comportamento duttile del materiale. Attraverso un software di analisi dell'immagine sono state misurate le zone della superficie di frattura caratterizzate dalla presenza di microcavità e per ciascuna area il diametro idraulico corrispondente. Tale parametro, definito come il rapporto tra il quadruplo dell'area ed il perimetro corrispondenti a ciascuna area, può essere considerato come un indice rappresentativo del grado di sinterizzazione del materiale in quanto durante la sinterizzazione i fenomeni diffusivi tendono ad estendere progressivamente i colli di collegamento tra i granuli di polvere già formati durante la fase di pressatura.

I risultati ottenuti mostrano che il materiale che presenta il maggior quantitativo di aree duttili è il materiale pre-legato contenente il 4% di nichel, mentre il minimo quantitativo è stato riscontrato per il materiale pre-legato contenente 0.9% di nichel. Le aree duttili delle polveri ibride mostrano valori tra loro simili ed intermedi rispetto a quelle dei materiali pre-legati. Inoltre il materiale da polvere ibrida con 4% di nichel diffusion-bonded mostra un valore di area duttile inferiore a quello del materiale pre-legato con il medesimo tenore di nichel. A questo proposito, maggiori informazioni possono essere tratte dai risultati relativi al calcolo del diametro idraulico. Mentre i materiali da polveri Distaloy DH-1, MSP 4 ed Atomet 4701 presentano aree di microcavità con diametro idraulico con valori tra loro molto prossimi, la polvere ibrida con 4% di nichel diffusion-bon-

ded è la sola che mostri un valore decisamente inferiore. Tale valore potrebbe essere correlato ad un'inadeguata diffusione del nichel: l'analisi del ciclo di sinterizzazione porta infatti a concludere che probabilmente 20-25 minuti di permanenza alla temperatura di sinterizzazione non sono sufficienti per far avvenire la diffusione degli elementi.

Tali risultati sono confermati dall'analisi microstrutturale. Il materiale da polvere Distaloy DH-1 è principalmente formato da martensite a differente morfologia: grossi aghi sono visibili su un fondo di aghi più fini. È presente inoltre austenite in via di trasformazione, unitamente a bainite superiore e perlite finissima, risolvibile solo al SEM.

Il materiale da polvere Distaloy HP-1 possiede un tenore di nichel tale da giustificare la presenza di una maggiore quantità di austenite (residua o in via di trasformazione), in prevalenza localizzata attorno ai pori. La martensite rimane ancora la principale fase presente, mentre la perlite fine è visibile solo in piccola quantità. La microanalisi EDS ha evidenziato la notevole eterogeneità chimica della matrice, specialmente per quanto riguarda il nichel. I più alti quantitativi di nichel e rame sono localizzati intorno ai pori, nelle zone caratterizzate dalla presenza di austenite residua seguite dalle zone interessate da austenite in via di trasformazione e da martensite. Il nichel ed il rame risultano completamente assenti nella perlite fine.

La microstruttura del materiale da polvere MSP 4 appare uniforme ed in prevalenza costituita da martensite fine; piccole quantità di austenite in via di trasformazione, omogeneamente distribuite, sono visibili spesso associate ad isole di perlite finissima.

Il materiale da polvere Atomet 4701 mostra una microstruttura costituita da zone di martensite, in cui sono stati evidenziati carburi di cromo e ferro, su un substrato di martensite associata ad austenite quasi completamente trasformata. Non è stata riscontrata austenite residua.

In conclusione, in concordanza con l'analisi microstrutturale, l'analisi frattografica mostra una notevole eterogeneità nella struttura del materiale da polvere Distaloy HP-1, confermando come la disomogeneità sia effettivamente una caratteristica peculiare degli acciai da polveri diffusion-bonded. Nei materiali pre-legati la microstruttura si presenta più uniforme e principalmente costituita da martensite con piccole quantità di austenite in via di trasformazione omogeneamente distribuite e completa assenza di austenite residua.